

Electronic Supplementary Information

Antibacterial and aqueous dual-responsive sensing activities of monomeric complexes with uncoordinated imidazole sites†

Lili Liang,^a Maomao Miao,^a Congsen Liu^a, Zihui Zong,^a Jun Zhang,^{*b} and Qiang Fang^{*a}

^aDepartment of Pharmaceutical Engineering, Bengbu Medical College, Bengbu, Anhui 233030, P. R. China.

^bSchool of Materials and Chemical Engineering, Anhui Jianzhu University, Hefei, 230601, P. R. China.

E-mail address:

fq333@souhu.com (Qiang Fang)

zhangjun@ahjzu.edu.cn (Jun Zhang)

Contents:

1. General procedures
2. TableS1 Selected Bond Lengths (Å) and Bond Angles (°) in **1-3**.
3. TableS2 Hydrogen bond lengths (Å) and bond angles (°) in **1-3**.
4. TableS3 The quenching constant K_{sv} or detection limit table of selected MOFs materials for Cu^{2+} and Hg^{2+} ions.
4. Figure S1 Powder XRD patterns of **1-3**.
5. Figure S2 TG-DSC curves of **1-3** under nitrogen.
6. Figure S3 Images of inhibition zones for **1-3** against *E. coli*, *S. aureus*, *Dysentery* and *Candida*.

General procedures: All reagents and solvents were of the analytical reagent grade (AR) and used without further purification. Infrared spectra were recorded on a NICOLET iS50 FT-IR spectrometer with a sample prepared as KBr discs in the range of 4000–400 cm^{-1} . ^1H NMR spectra of the ligand was recorded on a Varian mercury-plus 500 spectrometer. Elemental analyses (carbon, hydrogen, and nitrogen) were performed using a Perkin-Elmer 240C Elemental Analyzer. Powder X-ray diffraction (PXRD) patterns were collected in the 2θ range of 5° – 50° at a scan speed of 0.1°s^{-1} on a Bruker D8 diffractometer ($\text{Cu } K\alpha$, $\lambda = 0.154056 \text{ nm}$, 40 kV, 40 mA) at room temperature. Thermal gravimetric analysis (TGA) measurements were conducted on an STA 449-F5 thermal analyzer at a heating rate of $10^\circ \text{C}/\text{min}$ from 25°C to 700°C under a flux of nitrogen. Luminescence spectra for the solid and liquid samples were recorded on an LS-55 fluorescence spectrophotometer. The UV-Vis spectra of the ligand and 1-3 were obtained on a Thermo Evolution 220 UV-Visible Spectrophotometer.

Table S1 Selected Bond Lengths (\AA) and Bond Angles ($^\circ$) in **1-3**

1					
Co1-O1	0.2129(3)	Co1-O3	0.2109(2)	Co1-N3	0.2147(3)
Co1-N1	0.2216(3)	Co1-N4	0.2108(3)	Co1-N5	0.2114(3)
O1-Co1-N1	86.33(10)	O1-Co1-N3	88.32(10)	O3-Co1-O1	171.32(10)
O3-Co1-N1	85.88(9)	O3-Co1-N3	93.38(10)	O3-Co1-N4	91.97(10)
O3-Co1-N5	91.36(10)	N3-Co1-N1	75.03(10)	N4-Co1-O1	96.67(10)
N4-Co1-N1	147.67(10)	N4-Co1-N3	72.90(10)	N4-Co1-N5	76.77(11)
N5-Co1-O1	91.50(10)	N5-Co1-N1	135.47(11)	N5-Co1-N3	149.44(11)
2					
Cd1-O1	0.2403(4)	Cd1-O2	0.2578(4)	Cd1-O3	0.2336(4)
Cd1-N1	0.2476(4)	Cd1-N6	0.2366(4)	Cd1-N2	0.2437(4)
Cd1-N4	0.2287(4)				
O1-Cd1-N2	137.27(13)	N1-Cd1-O2	93.58(13)	O3-Cd1-N1	97.63(13)
O3-Cd1-N2	101.34(14)	O3-Cd1-N6	79.95(13)	O3-Cd1-O1	113.09(13)
O3-Cd1-O2	165.42(13)	N2-Cd1-N1	64.19(14)	N2-Cd1-O2	91.91(13)
N4-Cd1-O1	85.77(14)	N4-Cd1-N1	134.30(14)	N4-Cd1-N2	70.19(14)
N4-Cd1-O3	88.41(14)	N4-Cd1-N6	156.44(15)	N4-Cd1-O2	90.42(13)
N6-Cd1-O1	80.18(13)	N6-Cd1-O2	95.73(12)	N6-Cd1-N1	68.10(13)
N6-Cd1-N2	132.03(14)	O1-Cd1-O2	52.33(12)	O1-Cd1-N1	130.85(13)
3					
Ni1-O1	0.2084(4)	Ni1-O2	0.2099(4)	Ni1-N1	0.2141(5)
Ni1-N3	0.2053(5)	Ni1-N4	0.2042(5)	Ni1-N5	0.2155(5)
N1-Ni1-N5	128.62(19)	O2-Ni1-N5	88.08(18)	O1-Ni1-N5	88.76(18)
N3-Ni1-N5	153.60(19)	N4-Ni1-N5	78.10(19)	O2-Ni1-N1	88.12(18)

O1-Ni1-N1	89.30(18)	N3-Ni1-N1	77.78(19)	N4-Ni1-N1	153.18(19)
O1-Ni1-O2	173.38(17)	N3-Ni1-O2	93.72(18)	N4-Ni1-O2	90.87(18)
N3-Ni1-O1	91.69(18)	N4-Ni1-O1	94.17(19)	N4-Ni1-N3	75.54(19)

Table S2 Hydrogen bond lengths (Å) and bond angles (°) in **1-3**

Compound	D–H...A	d(D–H)	d(H...A)	d(D...A)	∠DHA
1	N2 ⁱ –H2 ⁱ ...O1	0.860	2.067	2.8457(2)	150.192(9)
	O3 ⁱⁱ –H3A ⁱⁱ ...O2	0.960	1.819	2.7768(3)	175.766(8)
	O3 ⁱⁱ –H3B ⁱⁱ ...N6	0.960	1.829	2.7685(2)	165.353(10)
2	N5–H5...O2 ⁱⁱⁱ	0.860	1.987	2.8161(4)	161.678(17)
	O3–H3A...N3 ^{iv}	0.850	1.935	2.7218(4)	153.335(17)
3	O1–H1A...O3 ^v	0.895	1.873	2.7616(19)	171.600(63)
	O2–H2B...O7 ^{iv}	0.934	1.949	2.8152(14)	153.314(54)
	O2 ⁱⁱⁱ –H2A ⁱⁱⁱ ...O6 ⁱⁱⁱ	0.935	1.989	2.9044(13)	165.883(53)
	N2–H2 ⁱⁱⁱ ...O6	0.880	2.281	3.0295(17)	142.854(54)
	N6 ^{iv} –H6 ^{iv} ...O3 ^v	0.880	2.033	2.8908(17)	164.43(6)

Symmetry codes: i = 1-x, 1-y, 2-z; ii = -1+x, 0.5+y, z; iii = 1-x, 1-y, 1-z; iv = 1.5-x, 0.5+y, 0.5-z; v = x + 1.5-y, 0.5+z; vi = -x, 0.5+y, 0.5-z.

Table S3 The quenching constant K_{sv} or detection limit table of selected MOFs materials for Cu^{2+} and Hg^{2+} ions.

MOFs	Target	Solvent	K_{sv} / M^{-1}	Detection Limit	Ref
[Eu(pdca) _{1.5} (dmf)] (DMF) _{0.5} (H ₂ O) _{0.5}	Cu^{2+}	DMF	89.4		15(a)
[H ₂ N(Me) ₂][Ln ₃ (L) ₂ (HCOO) ₂ (DMF) ₂ (H ₂ O)]	Cu^{2+}	DMF	2.35×10^3		15(d)
[Tb ₃ (L) ₂ (HCOO)(H ₂ O) ₅] DMF 4H ₂ O	Cu^{2+}	DMF	2.0218×10^3		9(b)
Eu ₂ (FMA) ₂ (OX)(H ₂ O) ₄ 4H ₂ O	Cu^{2+}	DMF	528.7		22(a)
{Mg(DHT)(DMF) ₂ } _n	Cu^{2+}	DMSO	170.2		24(a)
Eu(FBPT)(H ₂ O)(DMF)	Cu^{2+}	DMF	58.5		24(b)
{[Ln ₄ (μ ₃ -OH) ₄ (BPDC) ₃ (BPDCA) _{0.5} (H ₂ O) ₆]ClO ₄ 5H ₂ O} _n	Cu^{2+}	H ₂ O	344.9 ± 10.2		24(c)
[Cd ₂ (L)(OH)(H ₂ O) ₂] _n	Cu^{2+}	H ₂ O	3.09×10^4	6.66×10^{-7}	24(d)
[Cd(HL)(H ₃ CCOO)(H ₂ O) _n]	Cu^{2+}	H ₂ O	7.488×10^4	6×10^{-8}	Our work
	Hg^{2+}	H ₂ O	4.08×10^4	1.1×10^{-7}	
[TbL _{1.5} (H ₂ O) ₂] H ₂ O	Hg^{2+}	H ₂ O	7.465×10^3		25(a)
[Zn(2-NH ₂ bdc)(bipb)] _n	Hg^{2+}	H ₂ O	4.55×10^3	4.2×10^{-8}	25(b)
{[Cd(BIPA)(tfbdc)(H ₂ O)] DMF} _n	Hg^{2+}	DMF	1.27×10^4	1.2×10^{-7}	14(c)
[Zn(μ ₂ -1H-ade)(μ ₂ -SO ₄)] _n	Hg^{2+}	H ₂ O	7.7×10^3	7×10^{-8}	24(d)
{[Cd(BIPA)(IPA)] DMF} _n	Hg^{2+}	DMF	9.21×10^3	5×10^{-7}	23(b)
{[Cd(BIPA)(HIPA)] DMF} _n	Hg^{2+}	DMF	1.28×10^4	2.5×10^{-7}	
[Zn(OBA)(DPT) _{0.5}] DMF	Hg^{2+}	H ₂ O	3.737×10^3	1.8×10^{-6}	25(c)
	Hg^{2+}	CH ₃ CN	6.3618×10^4	6.9×10^{-6}	

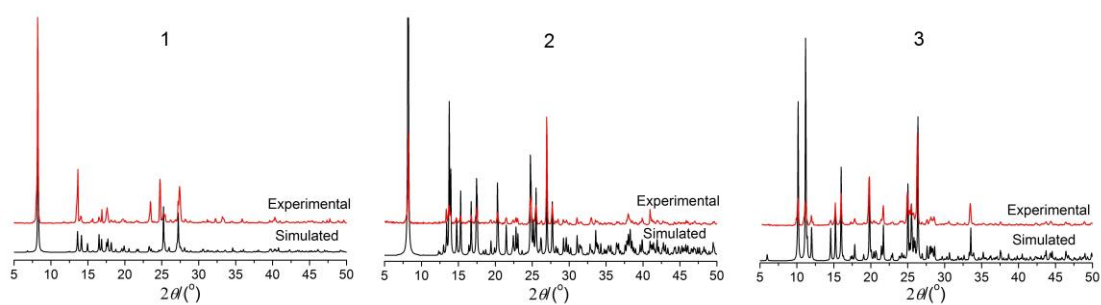


Figure S1 Powder XRD patterns of **1-3**

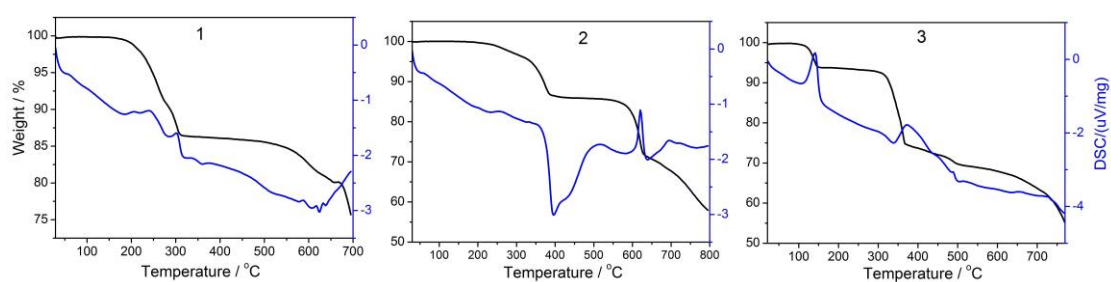


Figure S2 TG-DSC curves of **1-3** under nitrogen

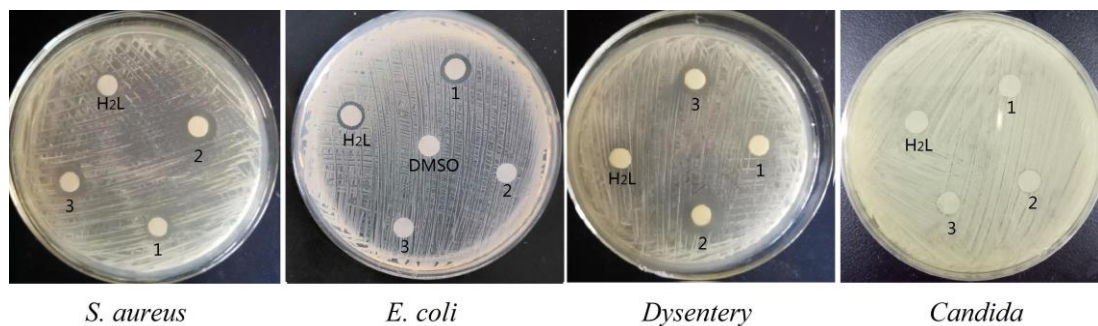


Figure S3 Images of inhibition zones for **1-3** against *E. coli*, *S. aureus*, *Dysentery* and *Candida*.